



RESEARCH ARTICLE

MODELLING & SIMULATION OF WIND ENERGY USING PMSG AND SOLAR PV SYSTEM FOR ELECTRICAL POWER GENERATION

*Satyajit Mohapatra and Namita Jaiswal

Electrical engineering, Sam Higginbottom University of Agriculture, Technology and Sciences, Allahabad, UP, India

ARTICLE INFO

Article History:

Received 22nd April, 2017
Received in revised form
17th May, 2017
Accepted 29th June, 2017
Published online 26th July, 2017

Keywords:

Photovoltaic system,
Converter (AC-DC),
Wind energy conversion system,
MPPT technology.

ABSTRACT

Due to ever increasing energy consumption, rising public awareness of environmental protection, and steady progress in power deregulation, alternative i.e., renewable distributed generation (DG) systems have attracted increased interest. Wind and photovoltaic (PV) power generation are two of the most promising renewable energy technologies. PV systems also show great potential in DG applications of the future due to their fast technology development and many merits they have, such as high efficiency, zero or low emission (of pollutant gases) and flexible modular structure. The modelling and control of a hybrid wind/PV/FC DG system is addressed in this paper. Different energy sources in the system are integrated through DC bus. Dynamic models for the main system components, namely, wind energy conversion system (WECS), PV energy conversion system (PVECS) and power electronic interfacing circuits are developed. Power control of a grid-connected PV and wind energy conversion system as well as load mitigation control of a stand-alone system is investigated. The pitch angle control for WECS and the maximum power point tracking (MPPT) control for PVECS are also addressed in the paper. Based on the dynamic component models, a simulation model for the proposed hybrid energy system has been developed using MATLAB/Simulink.

Copyright©2017, Satyajit Mohapatra and Namita Jaiswal. This is an open access article distributed under the Creative Commons Attribution License, which permits unrestricted use, distribution and reproduction in any medium, provided the original work is properly cited.

INTRODUCTION

With rising concerns about global warming and more since the last spike in oil prices that will cease to increase, renewable energy, long considered a useful adjunct course. Today, oil and gas are still relatively cheap. With the scarcity of raw materials, the price of fossil fuels will continue to rise. At the same time that renewable energy price should decrease mainly due to technological advances and production in larger series. This is why the PV and wind energy system have a great bright future in the forthcoming years. The PV and wind energy DC grid connected systems have become one of the most important applications of solar and wind energy (Madureira and PecasLopes, 2009; Majumder *et al.*, 2010; Chaouachi *et al.*, 2013). Different control strategy for three phase grid connected of PV modules and wind have been largely dealt with in the specialist literature in the last few years (see e.g. (Zhe Chen *et al.*, 2014; Yaow-Ming Chen *et al.*, 2006; Castaneda *et al.*, 2013; Galdi *et al.*, 2015)). Nevertheless, good integration of medium or large PV and Wind energy system in the grid may therefore require additional functionality from the inverter,

such as control of reactive power. Moreover, the increase in the average size of a PV system may lead to new strategies such as eliminating the DC-DC converter which is usually placed between the PV generator and DC-DC convertor, and moving the MPPT to the converter, which leads to increased simplicity, overall efficiency and a cost reduction.

System description and modelling

Solar Cell Model

a) Equivalent circuit of a solar cell

In order to analyze the electronic behaviour of a solar cell, an electrical equivalent model is considered. An ideal PV cell may be considered as a current source in parallel with a diode. In practice a PV cell is not ideal, so a shunt resistance and a series resistance component are added to the model. The resulting equivalent circuit is shown in the Figure 1,

b) Photovoltaic (PV) System

The most commonly used model for a PV cell is the one-diode equivalent circuit as shown in Figure 2.

*Corresponding author: Satyajit Mohapatra
Electrical engineering, Sam Higginbottom University of Agriculture,
Technology and Sciences, Allahabad, UP, India

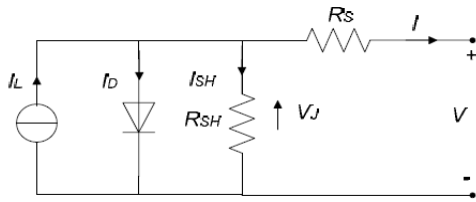


Fig. 1. Equivalent circuit

Since the shunt resistance R_{sh} is large, it normally can be neglected. The five parameters model shown in Figure2 (a) can therefore be simplified into that shown in Figure 2 (b). This simplified equivalent circuit model is used in this study

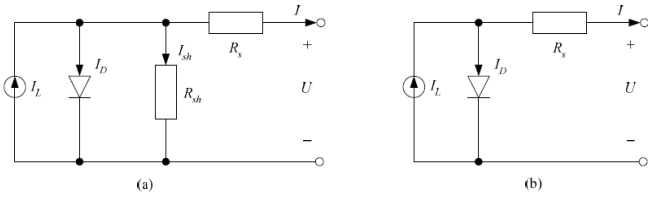


Figure 2. One-diode equivalent circuit model for a PV cell. (a) Five parameters model; (b) Simplified four parameters model

The relationship between the output voltage V and the load current I can be expressed as:

$$I = I_L - I_D = I_L - I_0 \left[\exp\left(\frac{U + IR_s}{\alpha}\right) - 1 \right] \dots\dots\dots (1)$$

- Where I_L = light current (A);
- I_0 = saturation current (A);
- I = load current (A);
- V = output voltage (V);
- R_s = series resistance (Ω);
- W = thermal voltage timing completion factor (V)

There are four parameters (I_L , I_0 , R_s and W) that need to be determined before the I-V relationship can be obtained. That is why the model is called a four-parameter model. Both the equivalent circuit shown in Figure 2(b) and the equation 1 look simple. However, the actual model is more complicated than it looks because the above four parameters are functions of temperature, load current and/or solar irradiance.

c) Characteristics of PV model

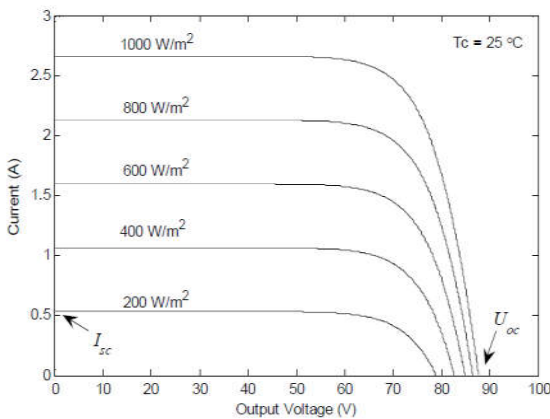


Figure 3. I-V characteristic curves of the PV mode under different irradiances

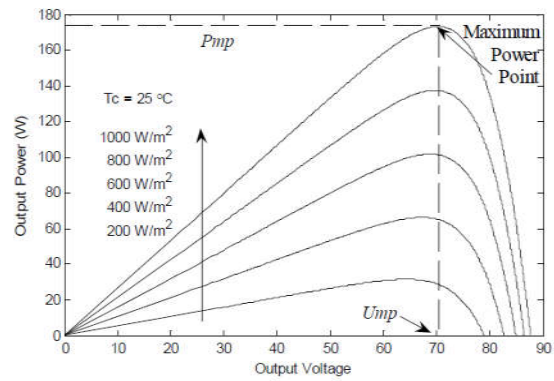


Figure 4. P-V characteristic curves of the PV model under different irradiances

d) Temperature Effect on the Model Performance

The effect of the temperature on the PV model performance is illustrated in Figures 4 and 5. From these two figures, it is noted that the lower the temperature, the higher is the maximum power and the larger the open circuit voltage. On the other hand, a lower temperature gives a slightly lower short circuit current.

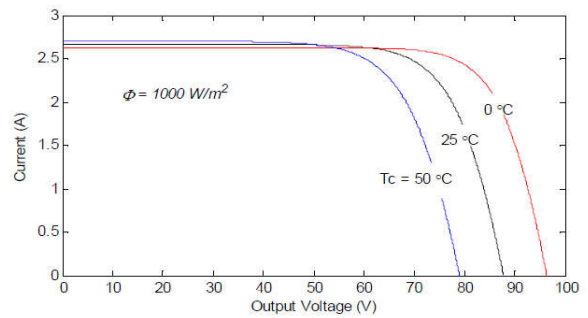


Fig. 4. I-V characteristic curves of the PV model under different temperatures

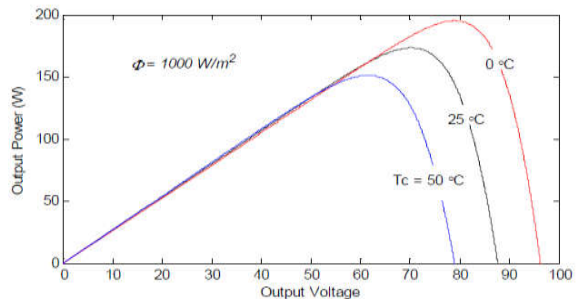


Figure 5. P-V characteristic curves of the PV model under different temperatures

Wind Energy System

a) Energy in Wind

Wind energy systems harness the kinetic energy of wind and convert it into electrical energy or use it to do other work, such as pump water, grains, etc. The kinetic energy of air of mass m moving at speed v can be expressed as,

$$E_k = \frac{1}{2}mv^2 \dots\dots\dots (2)$$

During a time period t , the mass (m) of air passing through a given area A at speed v is:

$$m = \rho Avt \tag{3}$$

where ρ is the density of air (kg/m^3).

$$P = \frac{1}{2} \rho Av^3 \tag{4}$$

The specific power or power density of a wind site is given as

$$P_{den} = \frac{P}{A} = \frac{1}{2} \rho v^3 \tag{5}$$

It is seen that the specific power of a wind site is proportional to the cube of the wind speed.

b) Power Extracted from Wind

The actual power extracted by the rotor blades from Wind is the difference between the upstream and the downstream wind powers

$$P = \frac{1}{2} k_m (v^2 - v_0^2) \tag{6}$$

where v is the upstream wind velocity at the entrance of the rotor blades, v_0 is the downstream wind velocity at the exit of the rotor blades and k_m is the mass flow rate, which can be expressed as

$$k_m = \rho A \frac{v + v_0}{2} \tag{7}$$

Where A is the area swept by the rotor blades.

From (6) and (7), the mechanical power extracted by the rotor is given by:

$$P = \frac{1}{2} \left[\rho A \frac{v + v_0}{2} \right] (v^2 - v_0^2) \tag{8}$$

Let

$$C_p = \frac{1}{2} \left(1 + \frac{v_0}{v} \right) \left[1 - \left(1 - \frac{v_0}{v} \right)^2 \right] \tag{9}$$

and rearrange the terms in (9), we have

$$P = \frac{1}{2} \rho Av^3 C_p \tag{10}$$

C_p is called the power coefficient of the rotor or the rotor efficiency. It is the fraction of the upstream wind power, which is captured by the rotor blades and has a theoretical maximum value of 0.59, shown in Figure 6. In practical designs, maximum achievable C_p is between 0.4 and 0.5 for high-speed, two-blade turbines and between 0.2 and 0.4 for low-speed turbines with more blades. It is noted from (6) that the output power of a turbine is determined by the effective area of the rotor blades (A), wind speed (v), and wind flow conditions at the rotor (C_p). Thus, the output power of the turbine can be varied by changing the effective area and/or by changing the flow conditions at the rotor system. Control of these quantities forms the basis of control of wind energy systems.

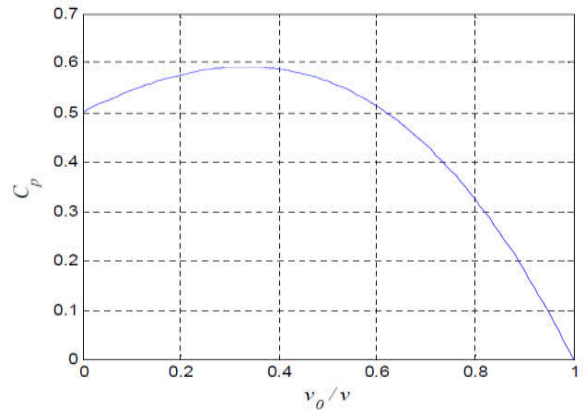


Fig 6. Theoretical rotor efficiency vs. v_0/v ratio

c) Tip Speed Ratio

The tip speed ratio (TSR), defined as the ratio of the linear speed at the tip of the blade to the free stream wind speed, is given as follows

$$\lambda = \frac{\omega R}{v} \tag{11}$$

where R is the rotor blade radius and ω is the rotor angular speed. TSR is related to the wind turbine operating point for extracting maximum power. The maximum rotor efficiency C_p is achieved at a particular TSR, which is specific to the aerodynamic design of a given wind turbine. For variable TSR turbines, the rotor speed will change as wind speed changes to keep TSR at some optimum level. Variable TSR turbines can produce more power than fixed TSR turbines.

d) Energy Conversion Systems (WECS)

Generally, there are two types of wind energy conversion systems: constant speed and variable speed systems, shown in Figure 7. In Figure 7 (a), the generator normally is a squirrel cage induction generator which is connected to a utility grid or load directly. Since the generator is directly coupled, the wind turbine rotates at a constant speed governed by the frequency of the utility grid (50 or 60 Hz) and the number of poles of the generator. The other two wind power generation systems, shown in Figure 7 (b) and (c), are variable speed systems. The generator is a doubly-fed induction generator (wound rotor). The rotor of the generator is fed by a back-to-back converter voltage source converter. The stator of the generator is directly

connected to load or grid. Through proper control on the converter for the rotor, the mechanical speed of the rotor can be variable while the frequency of output AC from the stator can be kept constant. Figure 7(c) shows a variable speed system which is completely decoupled from load or grid through a power electronic interfacing circuit. The generator can either be a synchronous generator (with excitation winding or permanent magnet), or an induction generator. In this dissertation, a variable speed WECS, similar to the one shown in Figure 7(b), is used for the hybrid energy system study. The generator used in the study is a self-excited induction generator.

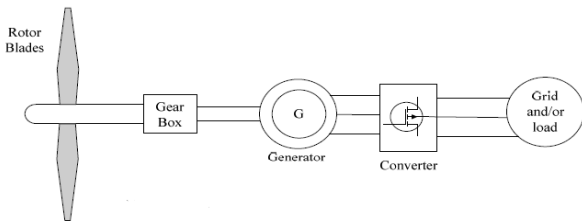


Fig. 7. (a) Constant and variable speed wind energy conversion systems

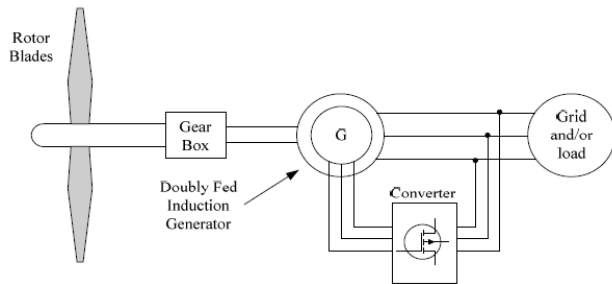


Fig. 7. (b) Constant and variable speed wind energy conversion systems

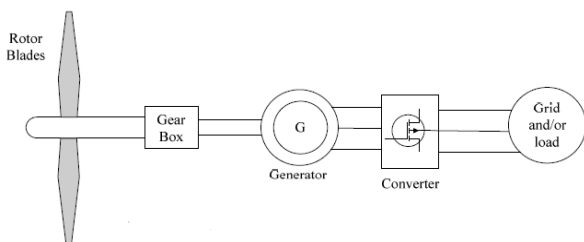


Fig. 7(c). Constant and variable speed wind energy conversion systems

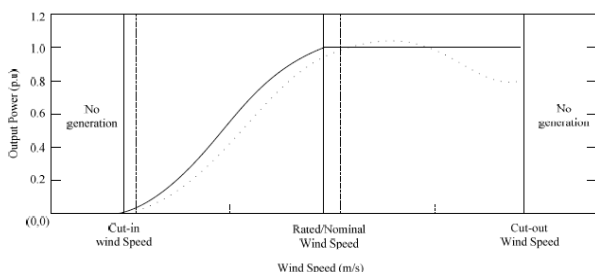


Fig. 8. Typical curves for a constant speed stall controlled (dotted) and variable

There are several ways to control the wind turbine output power. The two common ways to achieve this goal are: stall control and pitch control. For a stall controlled wind turbine, there is no active control applied to it. The output power is

regulated through a specifically designed rotor blades. The design ensures that when the wind speed is too high, it creates turbulences on the side of the rotor blades. The turbulences will decrease the aerodynamic efficiency of the wind turbine as a result. Pitch control is an active method which is used to reduce the aerodynamic efficiency by changing pitch angle (turning the rotor blades out of wind) of the rotor blades. It should be noted that the pitch angle can change at a finite rate, which may be quite low due to the size of the rotor blades. The maximum rate of change of the pitch angle is in the order of 3 to 10 degrees/second. It is noted from Figure 8 that a variable speed system normally has lower cut-in speed. The rated speed is also normally lower than a constant speed system. For wind speeds between the cut-in and the nominal speed, there will be 20-30% increase in the energy capture with variable speed compared to the fixed-speed operation, shown in Figure 8. For a pitch controlled wind system, the power for wind speeds over the nominal value can be held constant precisely. On the other hand, for a stall controlled constant speed system, the output power will reach its peak value somewhat higher than its rated value and then decreases as wind speed grows.

e) System Configuration

The configuration of the WECS system (Figure 9) studied in this paper is similar to the system shown in Figure 2(c). A PMSG, driven by a pitch controlled variable speed wind turbine acting as the prime mover, is used to generate electricity. The output AC voltage (with variable frequency) of the PMSG is rectified into DC and then a DC/AC inverter is used to convert the DC into 60 Hz AC. For stand-alone operation, an excitation compensating capacitor bank is necessary to start the induction generator. For grid-connected application, the compensating capacitor bank can be eliminated from the system. However, for a weak-grid, the reactive power consumed by the induction generator will deteriorate the situation. It is better to have a generation system with self-starting capability. Therefore, for the wind energy system studied in this paper, an excitation capacitor bank is always added regardless of the system being stand-alone or grid-connected. rectangle: the wind turbine together with the gear box and the PMSG.

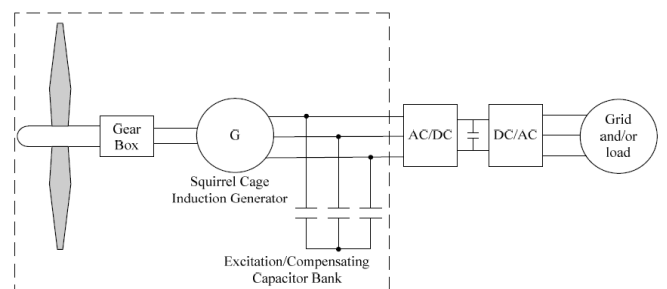


Fig 9. System block diagram of the WECS.

f) Wind Turbine Characteristics

The power P wind (in watts) extracted from the wind is given in equation 10. It is rewritten here as:

$$P_{wind} = \frac{1}{2} \rho A v^3 C_p(\lambda, \theta) \dots\dots\dots (12)$$

where T is the air density in kg/m³, A is the area swept by the rotor blades in m², v is the wind velocity in m/s. C_p is called the power coefficient or the rotor efficiency and is function of tip speed ratio and pitch angle (θ). The maximum rotor efficiency C_p is achieved at a particular TSR, which is specific to the aerodynamic design of a given turbine. The rotor must turn at high speed at high wind, and at low speed at low wind, to keep TSR constant at the optimum level at all times. For operation over a wide range of wind speeds, wind turbines with high tip speed ratios are preferred. In the case of the variable speed pitch-regulated wind turbines considered in this dissertation, the pitch angle controller plays an important role. Groups of C_p curves with pitch angle as the parameter obtained by measurement or by computation can be represented as a nonlinear function. The following function is used.

$$C_p = C_1(C_2 - C_3\theta - C_4) \exp(-C_5) \dots\dots\dots (13)$$

Where θ is the pitch angle.

Proper adjustment of the coefficients C1-C5 would result in a close simulation of a specific turbine under consideration. The values for C1-C5 used in this study are listed in Table1. The C_p-u characteristic curves at different pitch angles are plotted in Figure10. From the set of curves in Figure 10, we can observe that when pitch angle is equal to 2 degrees, the tip speed ratio has a wide range and a maximum C_p value of 0.35, suitable for wind turbines designed to operate over a wide range of wind speeds. With an increase in the pitch angle, the range of TSR and the maximum value of power coefficient decrease considerably.

Table 1. Parameter Values for C1-C5

C ₁	0.5
C ₂	116/k _θ
C ₃	0.4
C ₄	5
C ₅	21/k _θ

k_θ in Table1 used to calculate C2 and C5 is determined by u and θ as:

$$k_\theta = \left[\frac{1}{\lambda + 0.08\theta} - \frac{0.035}{\theta^3 + 1} \right]^{-1} \dots\dots\dots (14)$$

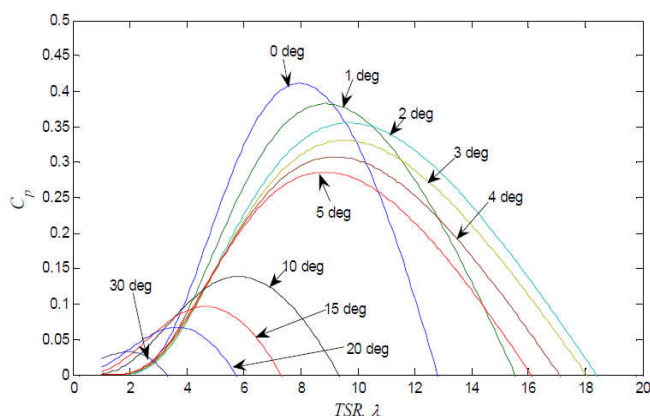


Fig. 10. Cp- characteristics at different pitch angles

For variable speed pitch-regulated wind turbines, two variables have direct effect on their operation, namely rotor speed and blade pitch angle. Power optimization strategy is employed when wind speed is below the turbine rated wind speed, to optimize the energy capture by maintaining the optimum TSR. Power limitation strategy is used above the rated wind speed of the turbine to limit the output power to the rated power. This is achieved by employing a pitch angle controller which changes the blade pitch to reduce the aerodynamic efficiency, thereby reducing the wind turbine power to acceptable levels, as discussed. The different regions of the above-mentioned control strategies of a variable speed wind turbine system are as shown,

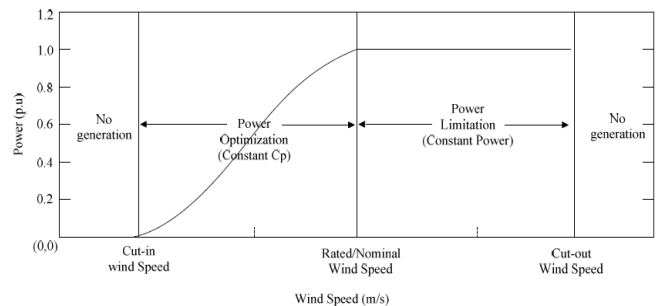


Fig. 11. Variable speed pitch controlled wind turbine operation regions

e. Pitch Angle Controller

The pitch angle controller used in this study employs PI controllers as shown in Figures. These controllers control the wind flow around the wind turbine blade, thereby controlling the torque exerted on the turbine shaft. If the wind speed is less than the rated wind speed, the pitch angle is kept constant at an optimum value. If the wind speed exceeds the rated wind speed, the controller calculates the power error (between the reference power and the output power of the wind turbine) and the frequency error (between the measured stator electrical frequency of the PMSG and the rated frequency). The output of the controllers gives the required pitch angle. In this figure, the Pitch Angle Rate Limiter block limits the rate of change of pitch angle as most modern wind turbines consist of huge rotor blades. The maximum rate of change of the pitch angle is usually in the order of 3o to 10o/second.

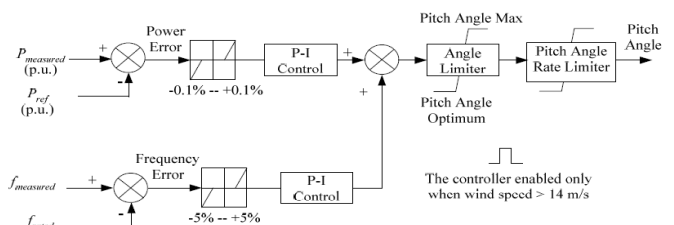


Fig. 12. Pitch angle controller

f. Variable-speed Wind Turbine Model

The dynamic model of the variable speed wind turbine are developed in MATLAB/Simulink. Figure 13 shows the block diagram of the wind turbine model. The inputs for the wind turbine model are, wind speed, air density, radius of the wind

turbine, mechanical speed of the rotor referred to the wind turbine side and power reference for the pitch angle controller. The output is the drive torque T drive which drives the electrical generator. The wind turbine calculates the tip speed ratio from the input Values and estimates the value of the power coefficient from the performance curves. The pitch angle controller maintains the value of the blade pitch at optimum value until the power output of the wind turbine exceeds the reference power input.

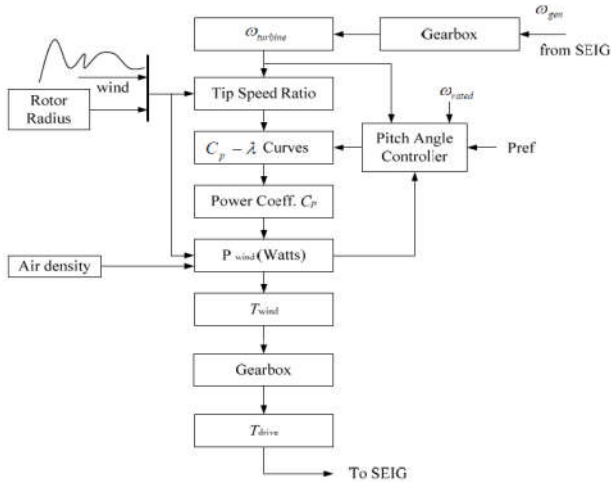


Fig. 13. Simulation model of the variable speed pitch-regulated wind turbine

g. Dynamic Model for PMSG

There are two fundamental circuit models employed for examining the characteristics of a PMSG. One is the per-phase equivalent circuit which includes the loop-impedance method adapted by Murthy et al and Malik and Al-Bahrani, and the nodal admittance method proposed by Ouazene and Mcherson and Chan. These methods are suitable for studying the machine’s steady-state characteristics. Another method is the dq-axis model based on the generalized machine theory proposed by Elderetal and Grantham et al, and is employed to analyze both the machine’s transient as well as steady-state.

h. Steady-state Model

Steady-state analysis of induction generators is of interest both from the design and operational points of view. By knowing the parameters of the machine, it is possible to determine its performance at a given speed, capacitance and load conditions. Loop impedance and nodal admittance methods used for the analysis of PMSG are both based on per-phase steady-state equivalent circuit of the induction machine, modified for the self-excitation case. They make use of the principle of conservation of active and reactive powers, by writing proper loop equations or nodal equations, for the equivalent circuit. These methods are very effective in calculating the minimum value of capacitance needed for guaranteeing self-excitation of the induction generator. For stable operation, excitation Capacitance must be slightly higher than the minimum value. Also, there is a speed threshold, the cutoff speed of the machine, below which no excitation is possible. In the following paragraph, a brief description of the loop impedance method is given for better understanding. The per-unit (p.u.) per-phase steady-state circuit of a self-excited induction

generator under lagging (RL) load is shown in Figures. In the analysis of PMSG, the following assumptions were made:

- Only the magnetizing reactance Xm is assumed to be affected by magnetic saturation, and all other parameters of the equivalent circuit are assumed to be constant. Self-excitation results in the saturation of the main flux and the value of Xm reflect the magnitude of the main flux. Leakage flux passes mainly in the air, and thus these fluxes are not affected to any large extent by saturation of the main flux.
- Per unit values of the stator and rotor leakage reactance (referred to stator side) are assumed to be equal ($X_{ls} = X_{lr} = X_l$). This assumption is normally valid in induction machine analysis.
- Core loss in the machine is neglected

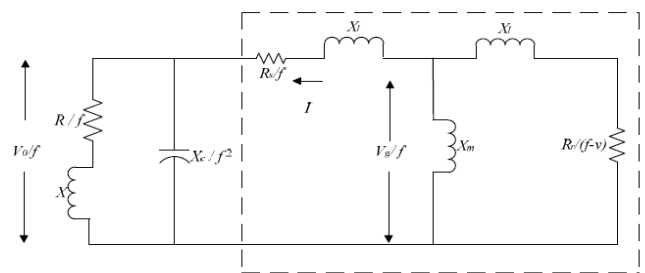


Fig.14. Equivalent T circuit of self-excited induction generator with R-L Load In the figure, the symbols are: Rs, Rr, R : p.u. per-phase stator, rotor (referred to stator) and load resistance respectively

Xl, X, Xm: p.u. per-phase stator/rotor leakage, load and magnetizing reactances (at base frequency), respectively.

Xc : p.u. per-phase capacitive reactance (at base frequency) of the terminal excitation Capacitor.

f, v : p.u. frequency and speed, respectively.

Vg, V0: p.u. per-phase air gap and output voltages, respectively. For the circuit shown in Figure 4.36, the loop equation for the current can be written as:

$$I Z = 0$$

Where Z is the net loop impedance given by

$$Z = \left(\frac{R_s}{f-v} + jX_l \right) \parallel jX_m + \frac{R_r}{f} + jX_l + \left(\frac{-jX_c}{f^2} \right) \parallel \left(\frac{R}{f} + jX \right) \dots \dots \dots (14)$$

For equations to hold true for any current I, the loop impedance (Z) should be zero. This implies that both the real and imaginary parts of Z are zero. These two equations can be solved simultaneously for any two unknowns, such as f and Xc.

Simulation result

a) Responses of the Model for the Variable Speed WECS:
The model of a 590 W variable speed wind energy

conversion system consisting of a pitch-regulated wind turbine and self-excited induction generator is developed in MATLAB/Simulink environment using SimPowersystems block-set.

Wind Turbine Output Power Characteristic

Figure 15 shows the wind turbine output power of the simulated model for different wind velocities. It can be observed that the output power is kept constant at higher wind velocities even though the wind turbine has the potential to produce more power. This is done to protect the electrical system and to prevent the over speeding of the rotor.

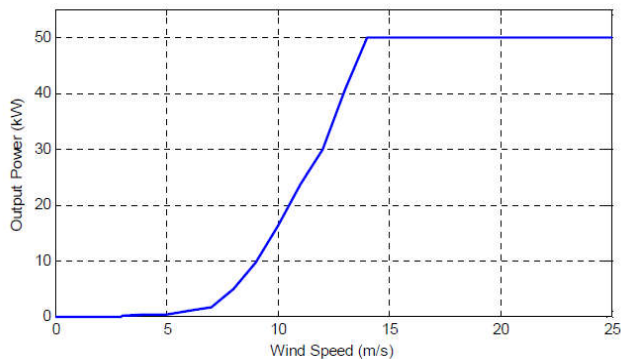


Fig 15. Wind turbine output power characteristic

Process of Self-excitation in PMSG

The process of self-excitation can occur only if there is some residual magnetism. For numerical method of integration, residual magnetism cannot be zero at the beginning of the simulation. Therefore, non-zero initial values are set for Kq and/or Kd, and the rotor speed. The process of voltage build up continues, starting with the help of the residual magnetism, until the iron circuit saturates and therefore the voltage stabilizes. In other terms, the effect of this saturation is to modify the magnetization inductance L_m , such that it reaches a saturated value; the transient then neither increases nor decreases and becomes a steady state quantity giving continuous self-excitation. The energy for the above process is provided by the kinetic energy of the wind turbine rotor. Figure shows the process of a successful self-excitation in an induction machine under no load condition with wind speed at 10m/s. The value of the excitation capacitor is given in the figure. An unsuccessful self-excitation process under the same condition (except a smaller capacitor bank) is shown in Figure.

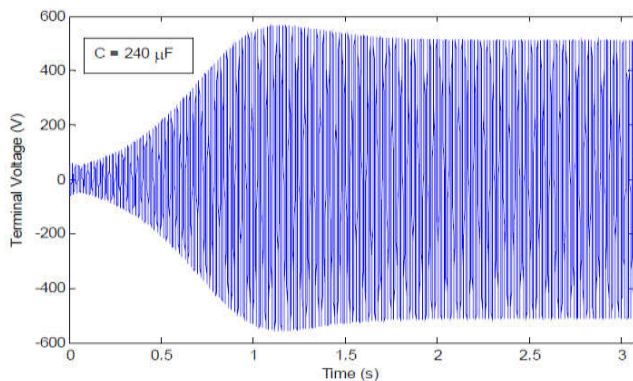


Fig. 16. A successful self-excitation process

Result obtained from wind turbine

This results show at input wind power is not constant so rotor speed is also fluctuating.

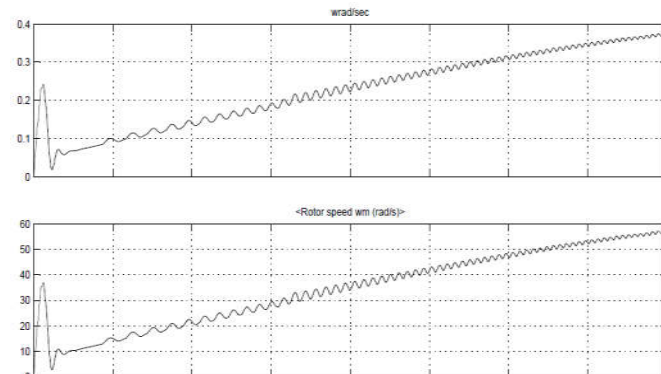


Fig. 19. Input wind speed

The fig. 20 given below shows the results of electromagnetic torque and mechanical torque of rotor

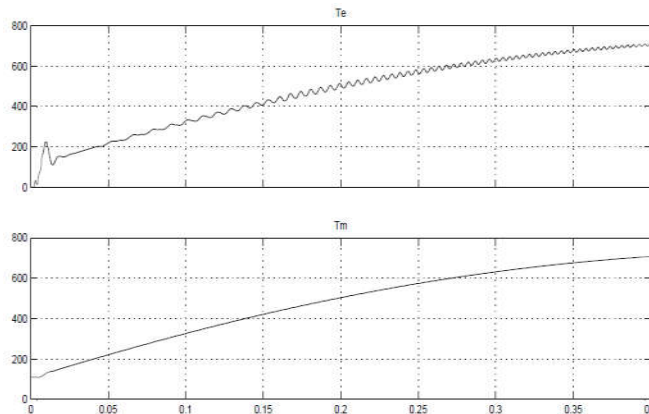


Fig. 20. Electrical and mechanical torque output

The fig 21 shows the line current and line voltage at output terminal of wind energy conversion system

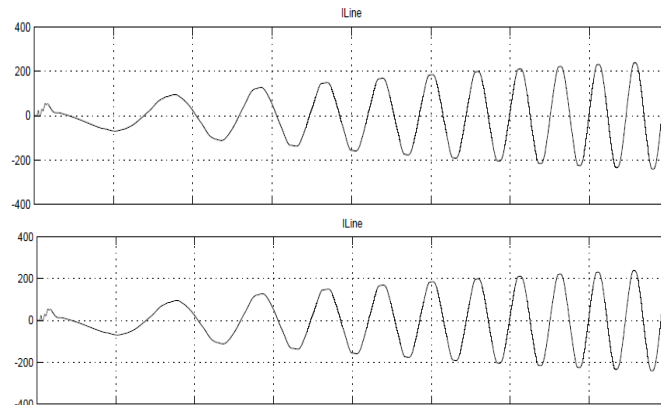


Fig. 21. Generator output voltage & current

Result obtained from hybrid system

This waveform show the output DC voltage when wind and solar systems are connected

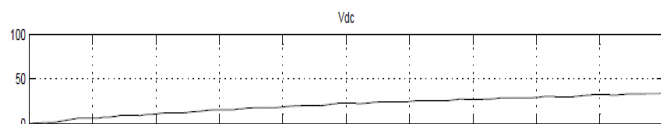


Fig. 22. DC output voltage of Hybrid system

This final load output voltage and current when all system is connected to grid.

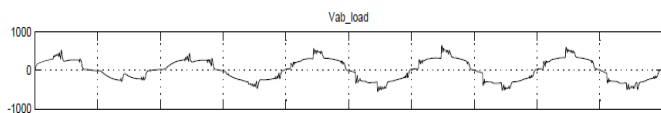


Fig. 23. Load voltage

REFERENCES

- Archie W. Culp, Jr., Principles of Energy Conversion, McGraw-Hill Book Company, 1979.
- Borowy, B.S. and Z.M. Salameh, "Methodology for optimally sizing the combination of battery bank and pv array in a wind/pv hybrid system," IEEE Trans. Energy Convers., vol.11, no.2, pp.367-375, Mar.1996.
- Castaneda M., Cano A., Jurado F., Sanchez H., Fernandez L. M., Sizing optimization, dynamic modelling and energy management strategies of a stand-alone PV/hydrogen/battery-based hybrid system, (2013), *International Journal of Hydrogen Energy*, Volume 38(10), pp.3830-3845.
- Chaouachi, A., R.M. Kamel, R. Andoulsi, and K. Nagasaka, "Multiobjective intelligent energy management for a microgrid," IEEE Trans. Ind. Electron., Vol.60, no.4, pp.1688-1699, Apr.2013.
- Galdi, V., A. Piccolo, P. Siano.: Dynamic Performances and Control of Dispersed Generators Connected through Inverter. In: Proceedings of international conference on modelling, control and automation and international conference on intelligent agents, web technologies and internet commerce, 2005, vol1, p1060-1065.
- Jitendra Kasera, Ankit Chaplot and Jai Kumar Maherchandani.: *Modelling and Simulation of Wind-PV Hybrid Power System using Matlab/Simulink*. In: Proceedings of Students Conference on Electrical, Electronics and Computer Science, SCEEC'S'12, 2012, pp. 1-4.
- Madureira, A.G. and J.A. Pecos Lopes, "Coordinated voltage support in distribution networks with distribution generation and microgrids," IET Renew Power Generation., vol.3, No.4, pp.439-454, Dec.2009.
- Majumder, R., B. Chaudhuri, A. Ghosh, R. Majumder, G. Ledwich, and F. Zare, "Improvement of stability and load sharing in an autonomous micro grid using supplementary droop control loop," IEEE Trans. Power Syst., Vol.25, No. 2, pp.768-808, May 2010.
- Manwell, J.F., J.G. McGowan and A.L. Rogers, Wind energy Explained – Theory, Design and Application, John Wiley & Sons, 2002.
- Marcelo, M. G. Villalva, J. R. Gazoli, E and Ruppert F. Modelling and Circuit-Based Simulation of Photovoltaic Arrays. In: Proceedings of power electronics conference COBEP'09, 2006, Brazil, p.1088-1094.
- Martin Kaltschmitt, Wolfgang Strechier, Andreas Wiese, "Renewable energy technology, economics and Environment" ISBN 978-3-540-70947-3. Springer Berlin Heidelberg, New York.
- Rekioua, D., Matagne, E. Optimization of photovoltaic power systems: Modelization, Simulation and Control (2012) Green Energy and Technology.
- Steven S. Zumdah, Chemical Principles, 2nd Edition, DC Heath and Company, Toronto, 1995.
- Yaow-Ming Chen, Chung-Sheng Cheng, and Hsu-Chin Wu. *Grid-Connected Hybrid PV/Wind Power Generation System with Improved DC Bus Voltage Regulation Strategy*. In: Proceedings of 21st annual applied power electronics conference and exposition APEC'06, 2006, pp.1088-1094.
- Zhe Chen, Frede Blaabjerg and Soeren Baekhoej Kjaer.: *Power Electronics as Efficient Interface in Dispersed Power Generation Systems*. In: IEEE Transactions on Power Electronics, 2004, vol. 19, no.5, p1184-1194.
